# Spherical Geometry Selection Used for Error Evaluation

Greg Hindman, Pat Pelland, Greg Masters
Nearfield Systems Inc.,
Torrance, CA 90502, USA
ghindman@nearfield.com, ppelland@nearfield.com, gmasters@nearfield.com

***Abstract*— Spherical near-field error analysis is extremely useful in allowing engineers to attain high confidence in antenna measurement results. NSI has authored numerous papers on automated error analysis and spherical geometry choice related to near field measurement results. Prior work primarily relied on comparison of processed results from two different spherical geometries: Theta-Phi ($0 \le \theta \le 180$, $-180 \le \phi \le 180$) and Azimuth-Phi ($-180 \le \theta \le 180$, $0 \le \phi \le 180$). Both datasets place the probe at appropriate points about the antenna to measure two different full spheres of data; however probe-to-antenna orientation differs in the two cases. In particular, geometry relative to chamber walls is different and can be used to provide insight into scattering and its reduction.**

**When a single measurement is made which allows both axes to rotate by 360 degrees both spheres are acquired in the same measurement (redundant). They can then be extracted separately in post-processing. In actual fact, once a redundant measurement is made, there are not just two different full spheres that can be extracted, but a continuum of different (though overlapping) spherical datasets that can be derived from the single measurement. For example, if the spherical sample density in Phi is 5 degrees, one can select 72 different full sphere datasets by shifting the start of the dataset in increments of 5 degrees and extracting the corresponding single-sphere subset. These spherical subsets can then be processed and compared to help evaluate system errors by observing the variation in gain, sidelobe, cross pol, etc. with the different subset selections.**

**This paper will show the usefulness of this technique along with a number of real world examples in spherical near field chambers. Inspection of the results can be instructive in some cases to allow selection of the appropriate spherical subset that gives the best antenna pattern accuracy while avoiding the corrupting influence of certain chamber artifacts like lights, doors, positioner supports, etc.**

## I. Introduction

The NIST 18-term error assessment originally developed for planar near-field measurements [1]has been adapted for spherical near-field (SNF) systems [2]and provides an accurate measure of the uncertainty in a particular SNF measurement. Once particular measurement errors are known, steps can be taken to reduce their impact on far-field radiation patterns. One of the most common and impactful sources of error in spherical near-field measurements is the presence of chamber multipath. One particularly effective technique for evaluating multipath in spherical measurements is the use of a double-sphere measurement [3]. Double-sphere measurements provide a way of comparing and/or averaging data acquired with AUT illuminating opposite points in the chamber between the two spheres. Recently, this technique has been extended to allow greater detail to be gleaned from the double-sphere measurements. This technique has been named "Phi Filtering" and this paper will discuss the implementation and effectiveness of this technique.

## II. History of the Use of Double-Sphere Measurements

Typical antenna measurements taken in a spherical Theta-Phi coordinate system move the probe relative to the antenna-under-test (AUT). To measure the full sphere, the Theta ($\theta$) or Phi ($\varphi$) coordinate needs to move over 360 degrees (double-sided) while the other coordinate need only rotate 180 degrees (one-sided). Examples of these would be:

$$-180 \le \theta \le +180,\ 0 \le \varphi \le +180 \ (\theta\text{: double-sided})$$

$$0 \le \theta \le +180,\ -180 \le \varphi \le +180 \ (\varphi\text{: double-sided})$$

If we allow both Theta and Phi to rotate a full 360 degrees each then the probe and AUT move relative to each other over a double sphere.

$$-180 \le \theta \le +180,\ -180 \le \varphi \le +180 \ (\theta,\varphi\text{: double-sided})$$

Double-sphere techniques for evaluating multipath have been discussed in previous AMTA papers [3], [4], [5]. When a double-sphere measurement is performed, various subsets of the double-sphere can be extracted to be transformed to the far-field individually, or can be averaged with other single-spheres and then transformed to the far-field.

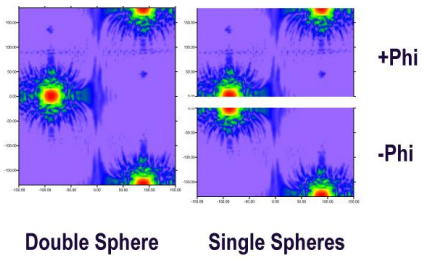


Figure 1. Near-Field Amplitude Distribution for a Double-Sphere Measurement (Left) and Two Single-Sphere Subsets

Figure 1. shows a double-sphere of data on the left and two subsets of that double-sphere on the right. First, the single-sphere labeled "+Phi" corresponds to the region where $-180 \le \theta \le +180$, $0 \le \varphi \le +180$. Similarly, the single-sphere labeled "-Phi" corresponds to the region where $-180 \le \theta \le +180$, $-180 \le \varphi \le 0$. Both spheres of near-field data can be transformed to the far-field and the resulting difference between the two far-field datasets will be a function of room scattering. By coherently averaging the difference we can reduce the scattering effects.

## III. PHI FILTERING

Once a double-sphere of data is measured a single-sphere can be extracted by choosing a subset of that data with a measurement span of only 180 degrees in Phi. In the previous case (Figure 1. ) the two spheres considered were:

$$-180 \le \theta \le +180,\ 0 \le \varphi \le 180 \text{ (+Phi)}$$

$$-180 \le \theta \le +180,\ -180 \le \varphi \le 0 \text{ (-Phi)}$$

In fact, these are not the only single-spheres available to be extracted and transformed to the far-field. If we allow Phi to start at any angle and stop after a span of 180 degrees has been realized we can get a multitude of spheres by sliding the 180 degrees Phi-filter to different starting points. Figure 2. shows the case where the Phi-filter spans the region $-90 \le \varphi \le +90$. Each of these available Phi-filtered spheres can then be transformed to the far-field and compared to give greater detail of the multi-path environment. The number of available spheres depends on the near-field Phi sampling density used during the double-sphere acquisition.

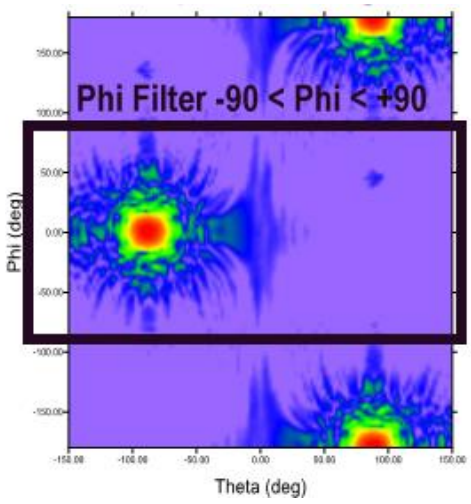


Figure 2. Phi-Filter Window Slid to Cover the Range -90 < Phi < +90

## IV. TEST CONFIGURATION

To evaluate the effectiveness of the Phi-filtering technique a set of tests was conducted using one of NSI's Theta-over-Phi SNF systems in a small anechoic chamber in the NSI laboratory (see Figures 3 thru 5). The NSI-700S-110 SNF test system allows measurements of small antennas up to 20 in (500 mm) in diameter over frequency ranges up to 100 GHz. Here, an X-band slotted waveguide array was mounted as AUT in equatorial mode so that its main beam illuminated the probe when (Theta, Phi) = (90 degrees, 0 degree) as shown in Figure 5.

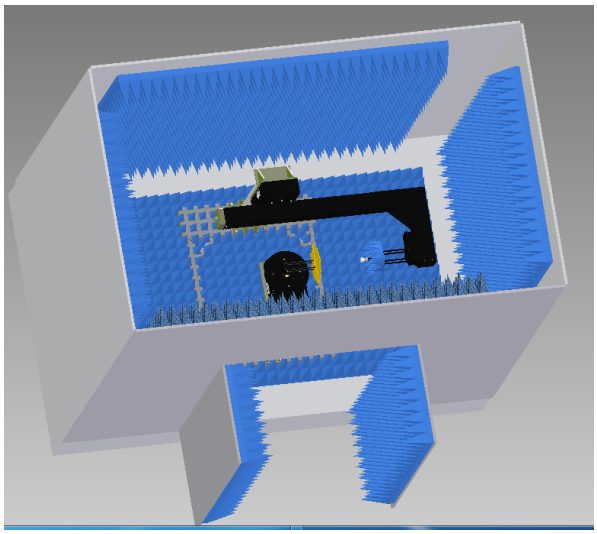

Figure 3. NSI-700S-110 SNF System in Anechoic Chamber Top View

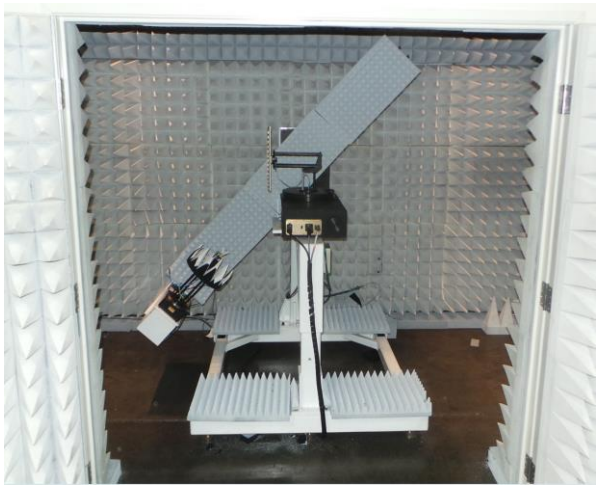

Figure 4. X-Band Slotted Waveguide Array Under Test on the NSI-700S-110 SNF System

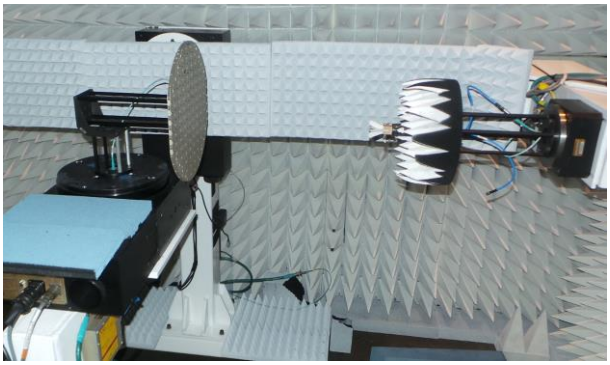

Figure 5. SWGA Mounted in Equatorial Mode with NSI Dual-Polarized Probe Mounted to Theta Swing Arm. (Phi=0° and Theta=90° Shown Here)

A partial double-sphere measurement was made over the range:

$$-165 \leq \theta \leq +165,\ -180 \leq \varphi \leq 180$$

Once the measurement was completed, the Phi-filter technique was employed to evaluate results obtained over multiple single-spheres by sliding the Phi-filter. Figure 6. shows four of these single-spheres where the Phi-filter is centered at Phi = 0, 90, 180, 270. For two of these single-spheres (0 degree, 180 degrees) the Phi-filter will be centered on the main beam of the SWGA's radiation pattern. The other two single-spheres (90 degrees, 270 degrees) will have the main beam split at the edges of the Phi span. The four single-spheres are outlined below:

$$-180 \leq \theta \leq +180,\ -90 \leq \varphi \leq 90 \text{ (0-centered)}$$

$$-180 \leq \theta \leq +180,\ 0 \leq \varphi \leq 180 \text{ (90-centered)}$$

$$-180 \leq \theta \leq +180,\ 90 \leq \varphi \leq -90 \text{ (180-centered)}$$

$$-180 \leq \theta \leq +180,\ -180 \leq \varphi \leq 0 \text{ (270-centered)}$$

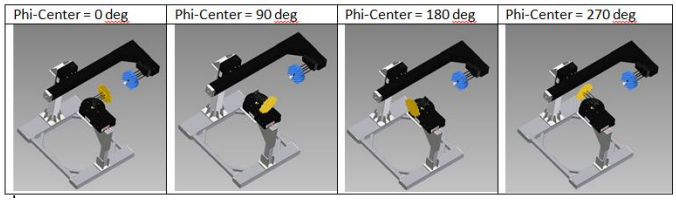


Figure 6. NSI-700S-110 SNF System Showing that Four Different Phi-Axis Positions of the SWGA ( Phi = 0°, 90°, 180°, 270°) Will Illuminate Different Walls of the Chamber

## V. Far-Field Pattern Results

Transformed far-field pattern data was processed with different Phi-filters to evaluate the effect on various antenna parameters. Sidelobe level, cross-pol, directivity, beam pointing and beamwidth were all evaluated for this study and were automatically calculated and tabulated using the Phi-filter routine. For this measurement, the sampling density was 2.5 degrees so data was transformed to the far-field using single-spheres with the filter sliding from 0 to 350 degrees in 25 degrees steps.

Figure 7. shows far-field Phi-cuts calculated using each of the extracted single-spheres. The pattern obtained from transforming the measured double-sphere is also overlaid as the bold, dashed curve. The results shown clearly indicate that sidelobe variations are present when different single-spheres are compared. This pattern variation is a result of the AUT (mounted here in equatorial mode) illuminating different parts of the chamber and scanner with different Phi-filters applied.

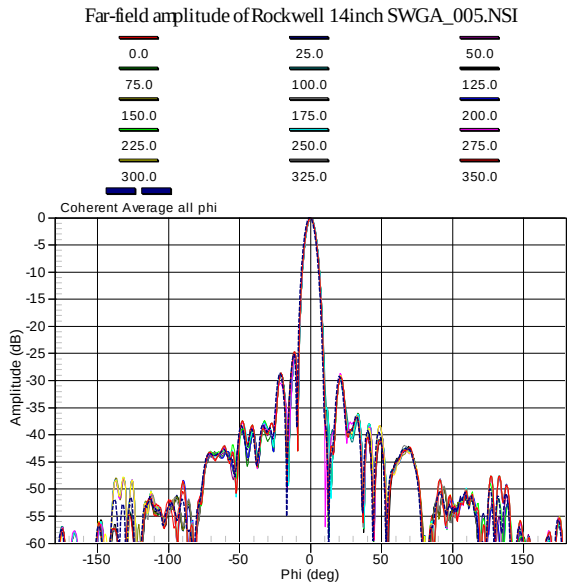


Figure 7. Multiple Far-Field Main Component Phi-Cuts Resulting from Different Single-Spheres with Sliding Phi-Filter Center

While the NSI2000 software and Phi-filter routine transform the single-sphere datasets to the far-field, they also automatically export a table summarizing the variation of other parameters of interest. This summary allows the range operator to identify the location of scattering bodies in the chamber and to either perform the necessary physical adjustments or acquire data over a Phi range that excludes the largest multipath effects

The first sidelobe on the plus and minus sides of the main beam were also chosen for closer analysis to quantify the variation resulting from this Phi-filter experiment. The first minus and plus sidelobes are located at roughly Phi = -11 degrees and +21 degrees, respectively. Figure 8. shows the far-field amplitude at these positions for datasets transformed using the same set of Phi-filters described above.

The variation in sidelobe amplitude evident in Figure 8. is a result of differences in multipath effects when the AUT points to different parts of the chamber. As the Phi-filter slides over the available filter range various scattering bodies in the chamber (walls, door, scanner, etc.) become more or less evident. For example, the largest variation for the right SLL appears when the Phi-filter is centered close to Phi = 270 degrees. At this position, the AUT is pointed at the scanner's swing arm, the closest scattering body in the chamber.

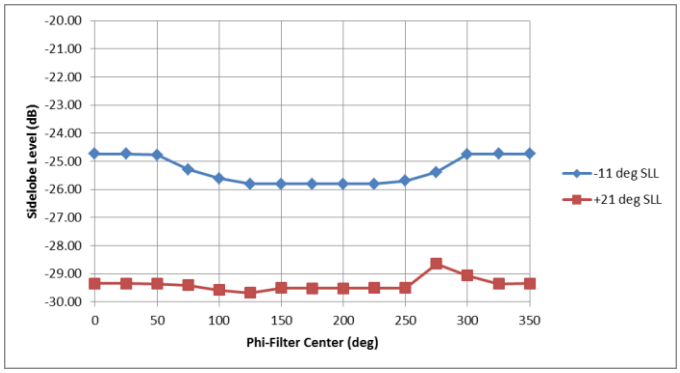


Figure 8. Sensitivity of Phi-Filter Window Center on First SLL on LHS and RHS

Next, the same set of Phi-filters was used to analyze the array's cross-polarized pattern. Figure 9. shows the resulting far-field plots overlaid along with the bold, dashed double-sphere average. Once again, variations are observed in the amplitude vs. Phi angle and these variations can be attributed to differences in the scattering environment as the Phi-filter slides.

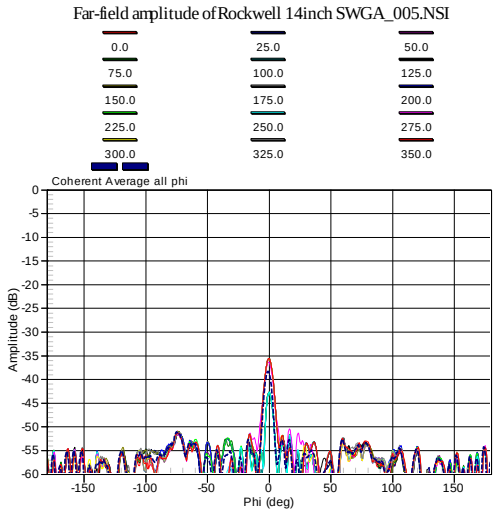


Figure 9. Multiple Far-Field Cross Component Phi-Cuts Resulting from Different Single-Spheres with Sliding Phi-Filter Center

As the NSI2000 processing also exports other parameters, we can review and analyze additional details. See Figure 10. thru Figure 12. for the resulting variations for peak directivity, 3 dB beamwidth, and beam pointing.

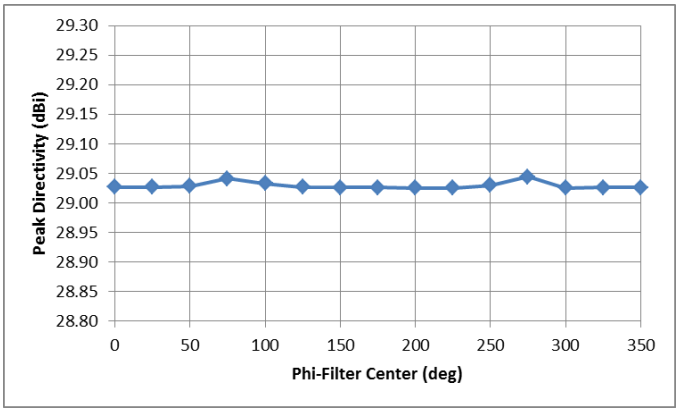


Figure 10. Peak Directivity Calculated using Various Phi-Filter Positions

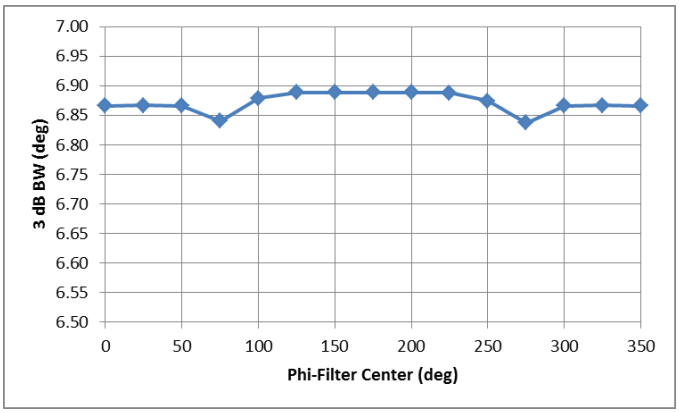


Figure 11. 3 dB Beamwidth Calculated using Various Phi-Filter Positions

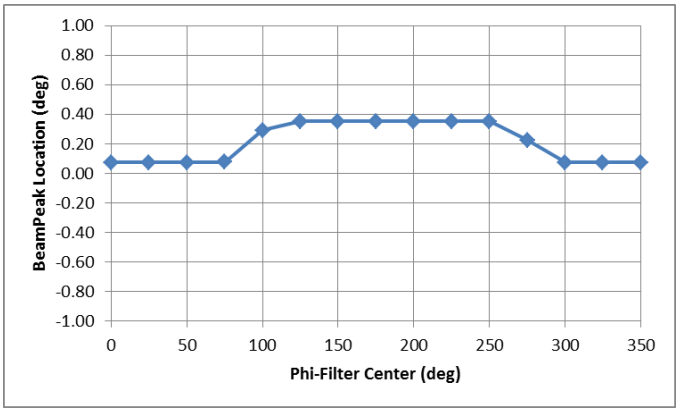


Figure 12. Beam Peak Location Calculated using Various Phi-Filter Positions

## VI. Summary of Measurement Uncertainties

Based on the results of the different single-spheres transformed with the sliding Phi-filter window, one can assemble a table of measurement uncertainties for a number of parameters. A vector average of all the sphere calculations is used, and then the uncertainty is calculated as the standard deviation of the multiple sphere results. Table I. below shows the resulting uncertainties.

TABLE I. Uncertainty Variation Derived from Phi-Filter Processing

| Parameter | Value | Uncertainty |
|---|---|---|
| LHS first SLL at -11° | -25.35 dB | ±0.48 dB |
| RHS first SLL at 21° | -29.39 dB | ±0.24 dB |
| Directivity | 29.03 dBi | ±0.01 dB |
| Azimuth 3 dB Beamwidth | 6.87° | ±0.02° |
| Azimuth Pointing | 0.21° | ±0.13° |

## VII. Perturbation Studies

This technique can be used to intelligently choose which spheres to include in evaluation of AUT performance. For instance, certain parts of an anechoic chamber like the absorber coverage of the door may induce higher reflections. To illustrate this idea more clearly, a gross error was introduced by leaving one of the chamber doors open during a measurement of the SWGA. The plot on the left of Figure 13. shows the near-field amplitude response of the double-sphere measurement performed with the chamber door open. In this image, the effects of room scattering are very evident in the range of $0 \leq \varphi \leq 180$. The plot on the right shows a Phi cut comparing data acquired with the door open to known good data acquired with the door closed. The Phi angles corresponding to the location of the door show very large pattern corruption due to room scattering effects.

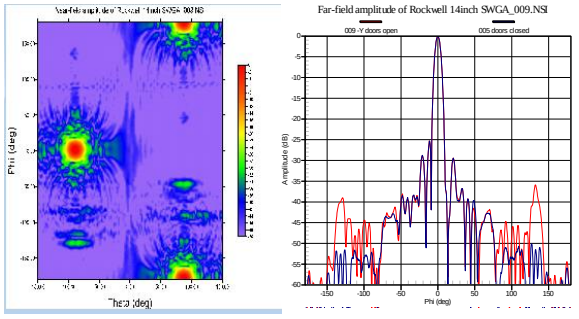


Figure 13. Near-Field Amplitude Response of Double-Sphere Measurement Performed with Door Open (Left) and Far-Field Pattern Results with Door Open and Closed (Right)

Using the Phi-filter technique, the range of $180 \leq \varphi \leq 360$ can be selected for processing, as shown in Figure 14. Now, the results acquired with the door open compare very favorably to those acquired with the door closed, provided the scattering region is filtered out.

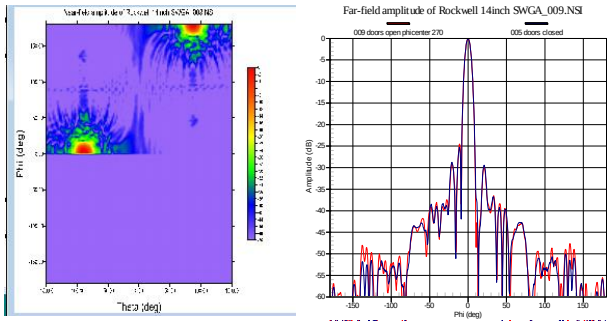


Figure 14. Near-Field Amplitude Response After Applying Phi-Filter Routine (Left) and Far-Field Pattern Results with Door Open and Closed (Right)

## VIII. Conclusion

This paper has shown a novel use of a double-sphere dataset for analyzing room scattering errors and minimizing them.

Once a double-sphere measurement is made, there are a continuum of different (though overlapping) spherical datasets that can be derived from the single measurement. These spherical subsets can be processed and then compared or averaged to help evaluate system errors by observing the variation in gain, sidelobe, cross pol, etc. with the different subset selections.

Inspection of the results can be instructive in some cases to allow selection of the appropriate spherical subset that gives the best antenna pattern accuracy while avoiding the corrupting influence of certain chamber artifacts like lights, doors, positioner.

## References


[1] A. Newell, "Error Analysis Techniques for Planar Near-Field Measurements", IEEE Trans Antennas & Propagation, AP-36, p. 581, 1988.

[2] G. Hindman, A. Newell, "Simplified Near-Field Accuracy Assessment", Proc. Antenna Measurement Techniques Association (AMTA) Annual Symp., 2006.

[3] G. Hindman, A. Newell, "Spherical Near-Field Self-Comparison Measurements", Proc. Antenna Measurement Techniques Association (AMTA) Annual Symp., 2004.

[4] G. Hindman & A. Newell, "Mathematical Absorber Reflection Suppression (MARS) for Anechoic Chamber Evaluation and Improvement", Proc. Antenna Measurement Techniques Association (AMTA) Annual Symp., 2008.

[5] Newell, Hindman, "Antenna Pattern Comparison Using Pattern Subtraction and Statistical Analysis", The 5th European Conference on Antennas and Propagation (EuCAP 2011)